JOC The Journal of Organic Chemistry

Note

pubs.acs.org/joc

Naphthotetrathiophene-Based Helicene-Like Molecules: Synthesis and Photophysical Properties

Xueqian Zhao,[†] Lipeng Zhang,[†] Jinsheng Song,*[,†] Yuhe Kan,[‡] and Hua Wang*[,†]

[†]National & Local Joint Engineering Research Center for Applied Technology of Hybrid Nanomaterials, Henan University, Kaifeng 475004, P.R. China

[‡]Jiangsu Province Key Laboratory for Chemistry of Low Dimensional Materials, School of Chemistry and Chemical Engineering, Huaiyin Normal University, Huaian 223300, China

Supporting Information

ABSTRACT: Two novel helicene-like molecules based on naphthotetrathiophene are successfully synthesized. All target molecules and intermediates are characterized by ^{1}H NMR, ^{13}C NMR, IR, and HRMS. Their electrochemical and photophysical properties are studied. The configurations of the molecules are optimized by DFT quantum calculations and UV−vis behaviors are also predicted to further understand the origin of different absorption bands. We believe the current work illustrated an efficient way for the design and synthesis of sophisticated structures with naphthotetrathiophene as building blocks.

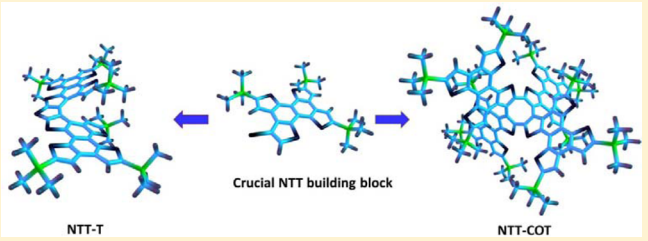

Helicenes and helicene-like molecules with ortho-fused aromatic rings are of great chiral properties and helical shape π-conjugated system,[1] which have been applied in chiral catalysts,[2] self-assembly,[3] chiroptical devices,[4] molecular recognition,[5] and molecular machines[6] during the past several decades. Rajca et al. have reported a series of synthetic work in preparing thiophene-based and carbon-based helicene-like molecules.[7] Our group has developed single-strand and double-strand helicenes from dithieno[2,3-*b*:3′,2′-*d*]thiophene.[8]

In literature, the modular building blocks to construct these beautiful thiophene-based helicenes and helicene-like molecules have developed from three fused-ring units (benzo[1,2-b:4,3-b′]dithiophene (**BDT**)[9] and dithieno[2,3-b:3′,2′-d]thiophene (**DTT**)[7,8]) to four fused-ring units (benzo[1,2-b:3,4-b′:5,6-b″]trithiophene (**BTT**)[10]) in Chart 1. However, the building blocks are still scanty and it is crucially important to explore novel modular units for the design of the helicene-like molecules.

Naphthatetrathiophene (**NTT**) with a planar structure brought effective extension of π-conjugation bearing six fused rings, exhibited strong aggregation, and indicated a significant potential as a cruciform scaffold for π-electron materials. It has been utilized for butterfly shaped molecules construction in our previous study.[11] In this article, **NTT** is again chosen as the basic and crucial building block to construct the single-strand and double-strand helicene-like molecules. Meanwhile, TMS groups are incorporated to assist the solubility of the molecules during the synthesis process. The spectroscopic and electrochemical data are collected; the HOMO, LUMO, and their absorption behaviors are further studied using the time dependent density functional theory (TD-DFT) calculation. The study of these beautiful and sophisticated structures is not only a good start to explore a new area that merges the planar and nonplanar π-systems together, but also a fundamental science of nonplanar aromatic compounds with extended

Chart 1. Thiophene-Based Building Blocks and Their Corresponding Helicene-Like Molecules

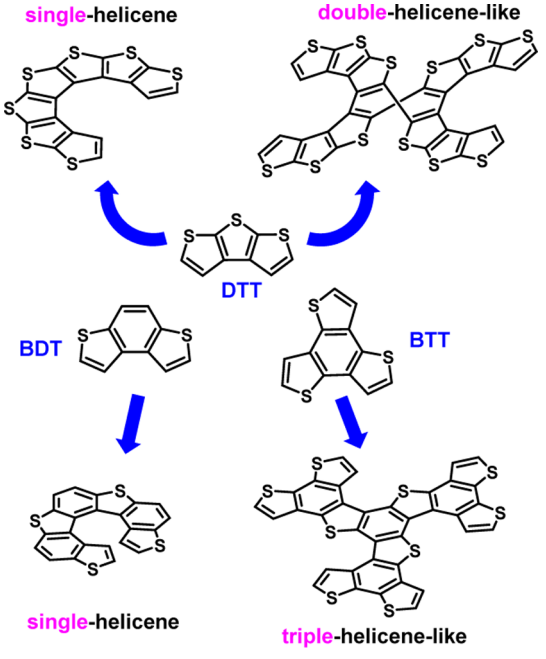

Received: March 9, 2016
Published: May 11, 2016

DOI: 10.1021/acs.joc.6b00502
J. Org. Chem. 2016, 81, 4856−4860

Scheme 1. Synthetic Routes of the NTT-Based Helicenes

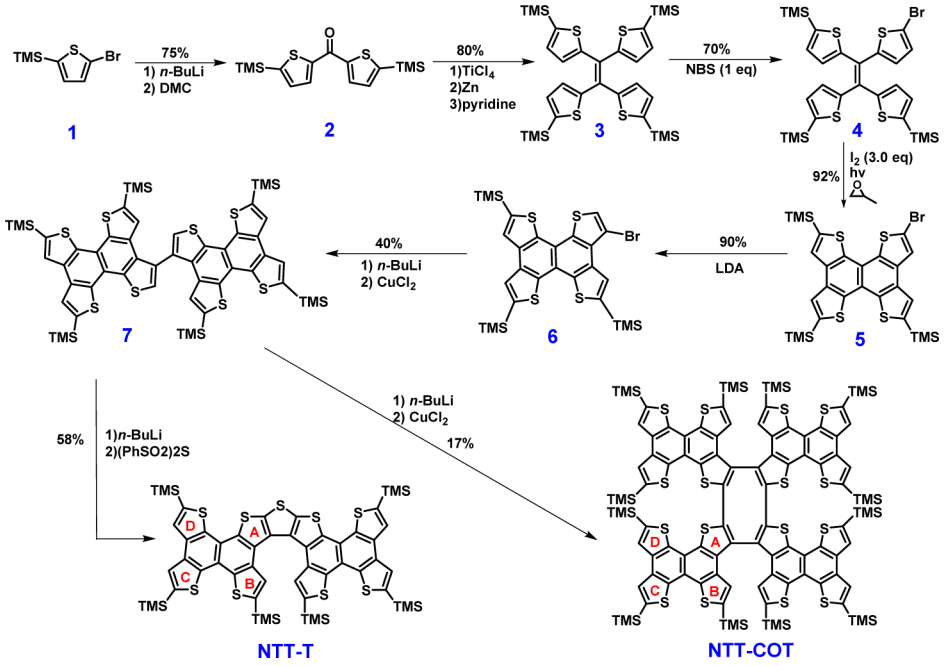

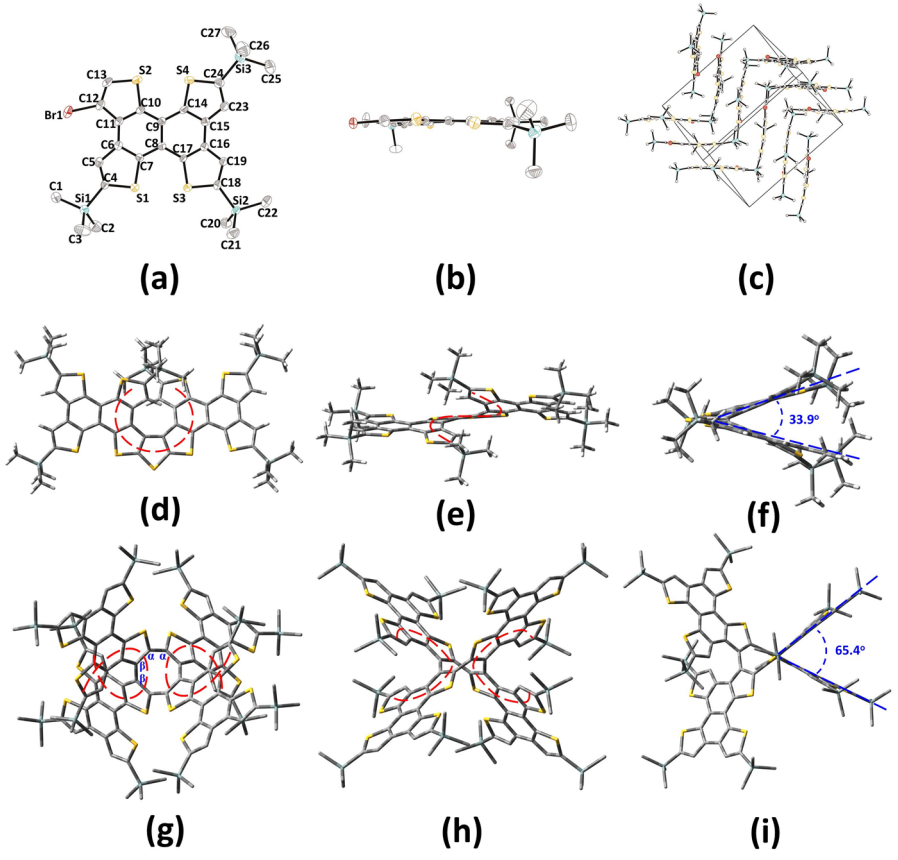

Figure 1. Crystal structures for **6** top view (a), side view (b), and the crystal packing (c). Carbon and sulfur atoms are depicted with thermal ellipsoids set at 30% probability level and all hydrogen atoms are omitted for clarity. The optimized molecular configurations of **NTT-T** and **NTT-COT** by theoretical quantum calculations: top view (d) and (g); front view (e) and (h); side view (f) and (i).

helical π-system, which might become a useful strategy for tuning molecular properties.

The synthetic route to of **NTT-T** and **NTT-COT** is shown in Scheme 1. Starting from 2-bromo-5-trimethylsilyl thiophene (**1**), bis(5-(trimethylsilyl)thiophen-2-yl)methanone (**2**) could be afforded in a yield of 75% via the Br/Li exchange in the presence of *n*-BuLi and quenching with *N*,*N*-dimethylcarbamyl chloride (DMC). Subsequently, the intermolecular McMurry

DOI: 10.1021/acs.joc.6b00502
J. Org. Chem. 2016, 81, 4856−4860

reaction of **2** is employed to generate tetrakis(5-(trimethylsilyl)-thiophene-2-yl)ethene (**3**) in a yield of 80%. Later, the selective monobrominated intermediate compound **4** is generated in the presence of *N*-bromosuccinimide (NBS). Under irradiation, the corresponding naphtho-unit (compound **5**) was obtained in high yield of 92% and via bromine dancing reaction, the crucial **NTT** building block (**6**) could be generated in a high yield of 90%. Then, the Br/Li exchange of compound **6** is carried out in the presence of *n*-BuLi and a **NTT** dimer (**7**) is generated via $CuCl_2$ oxidative coupling in a yield of 40%. Finally, the deprotonation of **7** is performed using *n*-BuLi, and the dilithiated intermediate was subsequently produced. When the reaction mixture is treated with $(PhSO_2)_2S$ or $CuCl_2$, the helicene-like molecules **NTT-T** or **NTT-COT** could be obtained in yields of 58 and 17%, respectively. The ^{1}H NMR analysis showed simple spectra with six singlet peaks for each **NTT**-based helicene-like molecule in Figures S9 and S14. Clearly, the three singlet peaks at downfield are attributed to the aromatic hydrogens from thiophene and the three singlet peaks at upfield are corresponded to methyl hydrogens at the TMS groups. However, the proton corresponding to the hydrogen atoms at ring B of **NTT-T** (δ 7.93) showed a large upfield shift to **NTT-COT** (δ 6.87), indicating a significant shielding upon the structure variation. All aim molecules and intermediates have been fully characterized by ^{1}H NMR, ^{13}C NMR, IR, and HRMS.

Fortunately, the molecular structure of the crucial building block **6** is confirmed by single crystal X-ray analyses shown in Figure 1a,b. It belongs to the monoclinic space group P2(1)/c. In **6**, all four thiophenes are almost in the same plane with the naphthalene core and S···H interactions are observed between the two neighbored molecules. In addition, its crystal packing structure is shown in Figure 1c. Unfortunately, the crystal structures of **NTT-T** and **NTT-COT** are not obtained, so a DFT calculation is conducted at B3LYP/6-31 G** level and the molecular configurations of both **NTT-T** and **NTT-COT** are optimized as shown in Figure 1d–i. In the case of **NTT-T**, it is clear that the bridge sulfur atom tries to drag the two **NTT** arms together to the same plane, but they are finally separated up and down with a dihedral angle of 33.9°, due to the steric hindrance of the end thiophene units and TMS groups. As for **NTT-COT**, which combines a cyclooctatetraene with four **NTT** arms, it is a little complicated but two helicene-like strands could be found simply (red dashed line in Figure 1g,h) and the **NTT** arms have more space to adjust their steric configuration. Meanwhile, different connection manners (α–α and β–β connections) between the thiophenes are found in **NTT-COT**, which results in conjugated and cross-conjugated structures at the same time in one molecule. At each single helicene-like strand of the two **NTT**-based molecules, **NTT-COT** presents more stretched configuration in space than that of **NTT-T** via the replacement of the sulfur atom by the saddle-shaped cyclooctatetraene core, which is also proved by the angles between the two **NTT** arms shown in Figure 1f and i.

All of the molecules are soluble in common organic solvents such as chloroform, dichloromethane, and tetrahydrofuran. UV–vis absorption spectroscopy was measured in solutions (5×10^{-6} M in dichloromethane) in Figure S20. Detailed photophysical characterization results of these **NTT** intermediates and helicene-like molecules are shown in Table 1. Obviously, compound **5** and **7** present very similar absorption curves and the peaks are shown around 314, 341, 355, 370, and 389 nm, respectively. However, the absorbance intensity of the **NTT**-dimer (**7**) is varied and the integrated absorbance of the dimer **7** is approximately 2-fold that of the monomer **5**. When the **NTT**-dimer is bridged by sulfur, i.e., a cross-conjugation is formed in **NTT-T**, significant bathochromic shift and lowered intensity are observed with a broad band including two weak peaks around 380 and 402 nm (Band I) and another strong broad absorption band at 328 nm (Band II). As for **NTT-COT**, which possesses four **NTT** arms and bridged by a cyclooctatetraene, it displays a similar absorption curve-shape, shares bands at similar positions, but varies at intensities when compared to **NTT-T** due to the elevated constitution of **NTT** units in each molecule. However, **NTT-COT** bears two cross-conjugated **NTT** dimer strands with the β–β connections in its molecular structure on the one hand; it possesses two conjugated dimer strands with the α–α connections in between the thiophenes on the other hand. This sophisticated structure endows **NTT-COT** with a red-shifted absorption onset and lowered band gap. In addition, the photoluminescence spectra of the helicene-like molecules are shown in Figure S20. **NTT-T** shows emissions at 405 and 427 nm, but **NTT-COT** displays bathochromic emissions at 463and 496 nm, which might attribute to the double conjugated and double cross-conjugated helicene-like structures in **NTT-COT**. These results also confirmed that the conjugated connection manners play predominant roles in the photoluminescence characterization.

Table 1. Summary of Optical and Electrochemical Properties of the NTT Molecules

compound	λ_{max} [nm]	λ_{onset} [nm]	E_g[a] [eV]	E_g^{cal}[d] [eV]	E_{ox} [V]	E_{HOMO}[b] [eV]	E_{LUMO}[c] [eV]
NTT-T	328	408	3.04	3.67	1.01	−5.79	−2.79
NTT-COT	322	421	2.95	3.42	1.09	−5.87	−2.92

[a] $E_g = 1240/\lambda_{onset}$. [b] $E_{HOMO} = -[E_{ox} - E_{(Fc/Fc+)} + 4.8]$. [c] $E_{LUMO} = E_{HOMO} + E_g$; E_{ox} vs $Ag/AgNO_3$ is measured in anhydrous CH_3CN/Bu_4F_6NP (0.1 M), $E_{(Fc/Fc+)}$ = 0.02 V and scan rate is 100 mV/s. [d] E_g^{cal} is the DFT calculated results.

To obtain further insight into the effect of molecular structure and electron distribution on the spectroscopic properties of these **NTT**-based helicene-like molecules, their electronic structure and excited-state calculations were performed by TD-DFT/PCM approach at the 6-31G (d, p) level. As shown in Figure S18, TD-B3LYP/PCM results could accurately reproduce the peak position and relative intensity of the measured whole absorption bands. The vertical excitation energies, oscillator strengths, and transition contributions of the most important states are presented in Table S1.

It is clear that the absorption band-I of **NTT-T** is attributed to the $S_0 \rightarrow S_1$ and S_3 excitations, which is mainly associated with the HOMO → LUMO transition and some other transitions, such as H-1 → LUMO and HOMO → L+1. Band-I of **NTT-COT** is also associated with the HOMO → LUMO transition, but the main contribution is originated from the H-1 → LUMO transition. For both **NTT**-based molecules, the observed band-II is ascribed to the mixed predicted transitions from higher energy excitations.

Their visualized of HOMO and LUMO distributions are shown in Figure 2. It is obvious that the electronic wave functions of both HOMO and LUMO are distributed almost entirely over the conjugated skeletons for both molecules and it is especially concentrated at the center of the cyclooctatetraene in **NTT-COT**. The HOMO of **NTT-T** and **NTT-COT** are

DOI: 10.1021/acs.joc.6b00502
J. Org. Chem. 2016, 81, 4856–4860

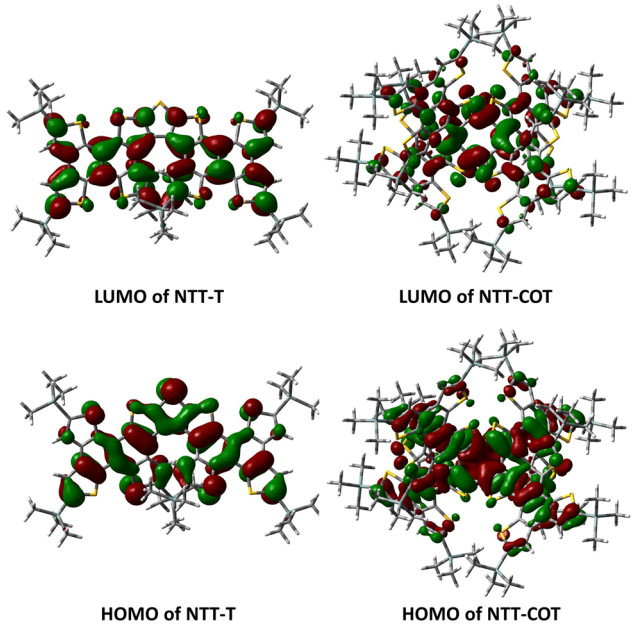

Figure 2. Visualized of HOMO and LUMO distributions at B3LYP/6-31G(d, p) for **NTT** based molecules.

mainly ascribed to the bonding of the C=C and most sulfur atoms of the **NTT** arms present contribution as well. Whereas at LUMO, the antibonding of the C=C is the main contributor; sulfur atoms are still observed with slight contribution in **NTT-T** molecules, but none participates the contribution to LUMO in **NTT-T** molecules.

Finally, the cyclic voltammetry (CV) are utilized to determine the electrochemical properties in thin film with $Ag/AgNO_3$ electrode as the reference electrode. Irreversible oxidation peaks are collected with the onset voltage of the first oxidation potentials as 1.01 and 1.09 V for **NTT-T** and **NTT-COT**, respectively in Figure S19; no redox process occurs at negative potential for these compounds. The HOMO energy levels of these compounds are calculated according to the onsets of the first oxidation, which are summarized in Table 1. The similar onset voltages of the oxidation peaks implies that the electrochemical properties of these **NTT**-based molecules are primarily dominated by the **NTT** units.

In summary, the basic **NTT** building block has been efficiently prepared with photochemical method and based on which, the single- and double-strand helicene-like molecules are designed and successfully synthesized. They all possess the helical structures, but **NTT-COT** also presents a larger saddle shape in its optimized configuration by DFT quantum calculation. Their spectroscopic and electrochemical properties are studied and **NTT-COT** present a red-shifted absorption onset and a lower band gap, which might be attributed to the better conjugation caused by the $\alpha-\alpha$ connection manner in between the thiophenes. In addition, DFT calculation is employed to deeply understand the contribution of different absorption bands in UV−vis spectra. In all, the current work illustrated an efficient way for the design and synthesis of sophisticated structures with the naphthotetrathiophene. We believe that the study of highly distorted helicene-like molecules will not only lay the groundwork in the growing realm of nonplanar π systems but also lead to the development of new functional materials.

EXPERIMENTAL SECTION

Materials and Instructions. All chemicals are purchased commercially and used without further purification. Compounds **1**−**5** are prepared according to our previous reported method.[11] Ether and tetrahydrofuran (THF) for use were freshly distilled from sodium/benzophenone prior to use. Concentration of *n*-BuLi (hexane) was determined by titration with *N*-pivaloyl-*o*-toluidine. Column chromatography was carried out on silica gel (300−400 mesh). Analytical thin-layer chromatography was performed on glass plates of silica gel GF-254 with detection by UV. ^{1}H and ^{13}C NMR spectra were obtained using chloroform-*d* ($CDCl_3$) as solvent and recorded on 400 MHz spectrometer. IR spectra were obtained using an FT-IR instrument, equipped with an ATR sampling accessory. HRMS spectra were recorded on a mass spectrometer equipped with TOF (EI^+). Melting point determination was taken on a melt-temp apparatus and was uncorrected. UV−vis spectra were obtained with a double-beam spectrophotometer at room temperature.

Synthesis of Compound ***6***. *n*-BuLi (2.46 M in hexane, 0.37 mL, 0.91 mmol, 1.5 equiv) was added dropwise to diisopropylamine (0.33 mL, 2.36 mmol, 1.7 equiv) in THF (7 mL) at 0 °C. After keeping 15 min at 0 °C, the fresh made LDA solution was transferred by syringe into a solution of **5** (0.4 g, 0.61 mmol) in THF (30 mL) at −30 °C. The reaction mixture was stirred at this temperature for 10 h, then methanol (excess) was added to quench the reaction. The organic layer was washed with water (3 × 30 mL) and dried over $MgSO_4$. After removing the solvent in vacuo, the residue was purified by column chromatography on silica gel with petroleum ether (60−90 °C)/$CHCl_3$ (8:1, v/v) as eluent to yield compound **6** (0.36 g, 90%) as a white solid. mp: 191−193 °C. ^{1}H NMR (400 MHz) δ 9.21(s, 1H), 8.18 (s, 2H), 7.84 (s, 1H), 0.57 (s, 9H), 0.57 (s, 9H), 0.54 (s, 9 H). ^{13}C NMR (100 MHz) δ 143.5, 143.0, 142.0, 140.2, 137.8, 137.0, 135.3, 135.3, 134.0, 133.7, 129.7, 129.5, 129.4, 128.9, 124.6, 121.1, 120.0, 107.3, 0.25, 0.20. HRMS (MALDI/DHB) Calcd for $C_{27}H_{31}Si_3S_4Br$, 645.9792, found: 645.9794 (M^+). IR (KBr): 2953, 2899 (C−H) cm^{-1}.

Synthesis of Compound ***7***. To a solution of **6** (0.0753 g, 0.11 mmol) in dry ethyl ether (20 mL), *n*-BuLi (1.0 eq, 0.6923 M, 0.17 mL in hexane) was added dropwise at −78 °C. After the mixture was stirred at −78 °C for 2 h, dry $CuCl_2$ (58 mg, 0.34 mmol, 3.00 equiv) was added, the reaction mixture was kept at −78 °C for 1 h, and then warmed up slowly to ambient temperature overnight. The reaction mixture was quenched with water and extracted with ethyl ether (3 × 30 mL). The organic layer was washed with water (3 × 20 mL) and then dried over $MgSO_4$. The white product **7** (0.025 g, 40%) was obtained by column chromatography on silica gel with petrol ether (60−90 °C) as eluent. mp > 300 °C. ^{1}H NMR (400 MHz, $CDCl_3$) δ 8.26 (s, 2H), 8.23 (s, 2H), 8.05 (s, 2H), 6.93 (s, 2H), 0.62 (s, 18H), 0.57 (s, 18H), −0.11 (s, 18H). ^{13}C NMR (100 MHz, $CDCl_3$) δ 143.1, 142.8, 141.8, 139.5, 138.1, 137.7, 135.1, 135.08, 134.6, 134.3, 134.1, 132.7, 129.8, 129.6, 129.5, 126.5, 121.1, 120.6, 0.26, 0.24, −0.56. HR-MS(MALDI/DHB) Calcd for $C_{54}H_{62}S_8Si_6$ 1134.1224, found:1134.1127 (M^+). IR (KBr): 2954, 2896 (C−H) cm^{-1}.

Synthesis of NTT-T. To a solution of **7** (0.102 g, 0.09 mmol) in dry ethyl ether (70 mL), *n*-BuLi (0.36 mL, 2.0 eq, 0.5 M in hexane) was added dropwise at −78 °C. After the mixture kept stirring at −78 °C for 2 h, dry $(PhSO_2)_2S$ (28.2 mg, 0.09 mmol, 1.0 equiv) was added. Then the reaction mixture was warmed up slowly to 50 °C and kept strring for 5 h. Finally, it was quenched with water at 0 °C and extracted with ethyl ether (3 × 30 mL). The organic layer was washed with water (3 × 30 mL) and then dried over $MgSO_4$. The **NTT-T** (0.060 g, 58%) was obtained as yellow solid by column chromatography on silica gel with petrol ether (60−90 °C) as eluent. mp > 300 °C. ^{1}H NMR (400 MHz, $CDCl_3$) δ 8.22 (s, 4H), 7.93 (s, 2H), 0.60 (s,18H), 0.58 (s,18H), 0.03 (s,18H). ^{13}C NMR (100 MHz, $CDCl_3$) δ 143.1, 143.0, 141.4, 140.0, 138.9, 138.3, 137.2, 137.0, 135.4, 135.0, 134.5, 134.3, 134.2, 129.7, 129.6, 127.1, 121.0, 121.0, 0.29, 0.21, −0.42. HR-MS (MALDI/DHB) Calcd for $C_{54}H_{60}S_9Si_6$:1164.0827, found: 1164.0792 (M^+). IR (KBr): 2955, 2893 (C−H) cm^{-1}.

Synthesis of NTT-COT. To a solution of **7** (0.154 g, 0.136 mmol) in dry ethyl ether (20 mL), *n*-BuLi (0.30 mL, 2.5 eq, 1.1364 M in

DOI: 10.1021/acs.joc.6b00502
J. Org. Chem. 2016, 81, 4856−4860

hexane) was added dropwise at −78 °C. After the mixture stirred at −78 °C for 2 h, dry $CuCl_2$ (138 mg, 0.816 mmol, 6.00 equiv) was added. Then the reaction mixture was warmed up slowly to ambient temperature and kept stirring for 48 h. Finally, the reaction mixture was quenched with water and extracted with ethyl ether (3 × 20 mL). The organic layer was washed with water (3 × 20 mL) and then dried over $MgSO_4$. The **NTT-COT** (0.027 g, 17%) was obtained as yellow solid by column chromatography on silica gel with petrol ether (60−90 °C)/$CHCl_3$ (4:1, v/v) as eluent. mp:157−160 °C. ^{1}H NMR (400 MHz, $CDCl_3$) δ 8.17 (s, 4H), 8.16 (s, 4H), 6.87 (s, 4H), 0.54 (s, 36H), 0.52 (s, 36H), −0.26 (s, 36H). ^{13}C NMR (100 MHz, $CDCl_3$) δ 143.3, 142.9, 141.6, 139.7, 138.0, 137.6, 135.6, 135.2, 135.0, 134.8, 134.5, 133.3, 130.2, 129.6, 129.4, 121.4, 120.2, 0.24, 0.21, −0.77. HRMS (MALDI/DHB) Calcd for $C_{108}H_{120}S_{16}Si_{12}$: 2264.2147, found: 2264.2148 (M^+). IR (KBr): 2962, 2893 (C−H) cm^{-1}.

■ ASSOCIATED CONTENT

Supporting Information

The Supporting Information is available free of charge on the ACS Publications website at DOI: 10.1021/acs.joc.6b00502.

^{1}H NMR, ^{13}C NMR, HRMS and IR data of all compounds; DFT calculation results of **NTT-T** and **NTT-COT**; UV−vis spectra of compound **5**, **7**, **NTT-T**, and **NTT-COT**; photoluminescence spectra of **NTT-T** and **NTT-COT**; and cyclic voltammetry scans of **NTT-T** and **NTT-COT** (PDF)

Crystallographic files of **6** (CIF)

■ AUTHOR INFORMATION

Corresponding Authors

*E-mail: songjs@henu.edu.cn.

*E-mail: hwang@henu.edu.cn.

Notes

The authors declare no competing financial interest.

■ ACKNOWLEDGMENTS

This research was supported by NSFC (21270255, U1204212, and 21404031), Program from Henan University (yqpy20140058), and Innovation Scientists and Technicians Troop Construction Projects of Henan Province (C20150011).

■ REFERENCES

(1) (a) Gingras, M.; Felix, G.; Peresutti, R. *Chem. Soc. Rev.* **2013**, *42*, 1007. (b) Gingras, M. *Chem. Soc. Rev.* **2013**, *42*, 968. (c) Shen, Y.; Chen, C. F. *Chem. Rev.* **2012**, *112*, 1463.

(2) (a) Crittall, M. R.; Rzepa, H. S.; Carbery, D. R. *Org. Lett.* **2011**, *13*, 1250. (b) Reetz, M. T.; Beuttenmüller, E. W.; Goddard, R. *Tetrahedron Lett.* **1997**, *38*, 3211. (c) Takenaka, N.; Chen, J.; Captain, B.; Sarangthem, R. S.; Chandrakumar, A. *J. Am. Chem. Soc.* **2010**, *132*, 4536.

(3) Kaseyama, T.; Furumi, S.; Zhang, X.; Tanaka, K.; Takeuchi, M. *Angew. Chem., Int. Ed.* **2011**, *50*, 3684.

(4) (a) Verbiest, T.; Sioncke, S.; Persoons, A.; Vyklický, L.; Katz, T. J. *Angew. Chem., Int. Ed.* **2002**, *41*, 3882. (b) Rajca, A.; Pink, M.; Xiao, S.; Miyasaka, M.; Rajca, S.; Das, K.; Plessel, K. *J. Org. Chem.* **2009**, *74*, 7504.

(5) (a) Weix, D. J.; Dreher, S. D.; Katz, T. J. *J. Am. Chem. Soc.* **2000**, *122*, 10027. (b) Wang, D. Z.; Katz, T. J. *J. Org. Chem.* **2005**, *70*, 8497.

(6) (a) Tani, Y.; Ubukata, T.; Yokoyama, Y.; Yokoyama, Y. *J. Org. Chem.* **2007**, *72*, 1639. (b) Wigglesworth, T. J.; Sud, D.; Norsten, T. B.; Lekhi, V. S.; Branda, N. R. *J. Am. Chem. Soc.* **2005**, *127*, 7272.

(7) (a) Rajca, A.; Miyasaka, M.; Pink, M.; Wang, H.; Rajca, S. *J. Am. Chem. Soc.* **2004**, *126*, 15211. (b) Rajca, A.; Miyasaka, M.; Xiao, S.; Boratynski, P. J.; Pink, M.; Rajca, S. *J. Org. Chem.* **2009**, *74*, 9105.

(8) Li, C.; Shi, J.; Xu, L.; Wang, Y.; Cheng, Y.; Wang, H. *J. Org. Chem.* **2009**, *74*, 408.

(9) Xiao, Q.; Sakurai, T.; Fukino, T.; Akaike, K.; Honsho, Y.; Saeki, A.; Seki, S.; Kato, K.; Takata, M.; Aida, T. *J. Am. Chem. Soc.* **2013**, *135*, 18268.

(10) (a) Dou, C.; Saito, S.; Gao, L.; Matsumoto, N.; Karasawa, T.; Zhang, H.; Fukazawa, A.; Yamaguchi, S. *Org. Lett.* **2013**, *15*, 80. (b) Fischer, E.; Larsen, J.; Christensen, J. B.; Fourmigue, M.; Madsen, H. G.; Harrit, N. *J. Org. Chem.* **1996**, *61*, 6997.

(11) (a) Wu, T.; Shi, J.; Li, C.; Song, J.; Xu, L.; Wang, H. *Org. Lett.* **2013**, *15*, 354. (b) Song, J.; Wu, T.; Zhao, X.; Kan, Y.; Wang, H. *Tetrahedron* **2015**, *71*, 1838.

DOI: 10.1021/acs.joc.6b00502
J. Org. Chem. 2016, 81, 4856−4860